



# Ultrasonic transducers based on curved lead-free piezoelectric thick films for high resolution medical imaging

Franck Levassort, Konstantin Astafiev, Rasmus Lou-Moeller, Jean-Marc Grégoire, Lise Nielsen, Wanda W. Wolny, Marc Lethiecq

## ► To cite this version:

Franck Levassort, Konstantin Astafiev, Rasmus Lou-Moeller, Jean-Marc Grégoire, Lise Nielsen, et al.. Ultrasonic transducers based on curved lead-free piezoelectric thick films for high resolution medical imaging. Société Française d'Acoustique. Acoustics 2012, Apr 2012, Nantes, France. 2012. <hal-00810928>

**HAL Id: hal-00810928**

**<https://hal.archives-ouvertes.fr/hal-00810928>**

Submitted on 23 Apr 2012

**HAL** is a multi-disciplinary open access archive for the deposit and dissemination of scientific research documents, whether they are published or not. The documents may come from teaching and research institutions in France or abroad, or from public or private research centers.

L'archive ouverte pluridisciplinaire **HAL**, est destinée au dépôt et à la diffusion de documents scientifiques de niveau recherche, publiés ou non, émanant des établissements d'enseignement et de recherche français ou étrangers, des laboratoires publics ou privés.





# ACOUSTICS 2012

## Ultrasonic transducers based on curved lead-free piezoelectric thick films for high resolution medical imaging

F. Levassort<sup>a</sup>, K. Astafiev<sup>b</sup>, R. Lou-Moeller<sup>b</sup>, J.-M. Grégoire<sup>a</sup>, L. Nielsen<sup>b</sup>,  
W.W. Wolny<sup>b</sup> and M. Lethiecq<sup>c</sup>

<sup>a</sup>Université François Rabelais de Tours, UMRS Imagerie et Cerveau, 10, boulevard Tonnellé,  
BP 3223, 37032 Tours Cedex 01, France

<sup>b</sup>Meggitt A/S, Hejreskovvej 18A, DK-3490 Kvistgaard, Denmark

<sup>c</sup>Université François Rabelais de Tours, GREMAN, ENIVL, Rue de la Chocolaterie BP 3410,  
41034 Blois, France

franck.levassort@univ-tours.fr

A pad-printing process was developed to deposit a curved KNN-based lead-free piezoelectric thick film for focused transducer applications, namely medical imaging. This thick film was directly deposited on a porous KNN electroded backing to deliver an integrated structure. The electromechanical properties of the piezoelectric thick film in thickness mode were deduced, with a  $k_t$  over 35%, which is comparable to those obtained with similar compositions deposited by a screen-printing process on flat alumina substrates. The corresponding focused transducer has a center frequency of 12 MHz, a relative bandwidth at -6dB over 90% and a f-number of 1.3 according to the chosen focal distance (around 5 mm). The transducer sensitivity was sufficiently high to be integrated in a mechanical probe of a high frequency echographic system. Images of human skin *in vivo* were then observed. To conclude, the replacement of lead-based high frequency transducers by "green" devices could be a viable option.

## 1 Introduction

Lead free ferroelectric materials are receiving much attention due to their high electromechanical properties for several compositions, such as the KNN family, that make them promising candidates to replace lead-based piezoceramics (typically PZT) that will eventually be banned by environmental regulations in many countries over the world and in particular in the European Union [1]. Several papers have given a list of possible compounds with high potential to substitute the PZT [2-4]. It has been demonstrated that non-textured doped KNN-based ceramics can deliver properties comparable to those of textured ceramics [5]. Moreover, KNN thick films are particularly well adapted for high frequency applications due to higher wave velocities than PZT and a dielectric constant in an acceptable range for single element transducers [6-9].

In this paper, a KNN based thick film is deposited on a curved substrate by pad-printing in order to be used in a focused high frequency transducer. The substrate used is a porous lead-free KNN cylinder specifically developed to exhibit the required acoustical properties of a backing (acoustical impedance, high attenuation...) and compatible with the high sintering temperature of the KNN thick film. In the following section, the fabrication of this integrated structure is described. The characterization of these structures [10] is reported in section 3 and results compared to those of screen-printed KNN-based thick films. Finally the two last sections present the fabricated transducers, their characterization and their integration in an echographic system to deliver *in vivo* skin images.

## 2 Structure fabrication

### 2.1 Porous lead-free substrate

A cylinder of unpoled lead-free KNN was first fabricated with a length of 10 mm and a radius of 3 mm. A spherical-shaped depression was then machined onto the top face of the cylinder using a lens grinder. The radius of curvature was chosen according to the desired focal distance (here around 5 mm) of the transducer. The porosity is introduced in this material for two main reasons. The first is to decrease the acoustical impedance of this substrate so it will be lower than that of the piezoelectric thick film. Secondly, the porosity content increases the attenuation in the material so it can be considered as a semi-infinite medium, by avoiding any back echoes even if its size is limited (to minimize the size of the transducer).

### 2.2 Lead-free pad-printed thick films

Doped  $(K_{0.5}Na_{0.5})NbO_3$  (KNN) based compositions obtained by conventional solid state synthesis and adapted to large scale production were processed. The synthesized KNN-based powder was mixed with organic vehicle and sintering aids in a mortar. The mixture was then put into a triple roller mill twice to obtain a homogeneous paste. Initially, the rheological properties of this paste were tuned (by adding solvents) for screen-printing process [11] but in this work, modifications were performed and specifically adapted for the pad-printing process.

The technology of pad-printing was used to deposit thick films on curved golded lead-free porous substrates. In a previous paper [12], the pad-printing process was already described. But to summarize, the print layout is etched into a steel plate (cliché) and the paste (or ink) is flooded over the cliché, then the excess paste is removed with a doctor blade leaving paste only in the etched structure. The paste is then transferred to the curved substrate with a silicone rubber pad, which picks up the paste from the cliché and deposits it onto the substrate. Thanks to the deformation of the silicone pad, printing process on three-dimensional surfaces is possible.

After printing, the organic vehicle is dried off in a ventilated and heated oven at around 100°C. For a fired thickness of about 50  $\mu\text{m}$ , several layers of KNN-based paste are successively printed. After printing of all the layers, the thick film is sintered at around 1000°C.

The pad-printing process was also used to deposit the two electrodes. For that, commercial gold (bottom electrode) and silver (top electrode) pastes were used. The samples were heat treated for 2 hours before they are mounted in a polarization holder and put into a ventilated oven at elevated temperature (> 90°C). Polarization was carried out with an electric field higher than 2 kV/mm for 10-15 minutes.

The final structure is shown in Figure 1. Two electrical contacts (from the bottom and top electrodes) were placed on the lateral face of the substrate to facilitate transducer fabrication.

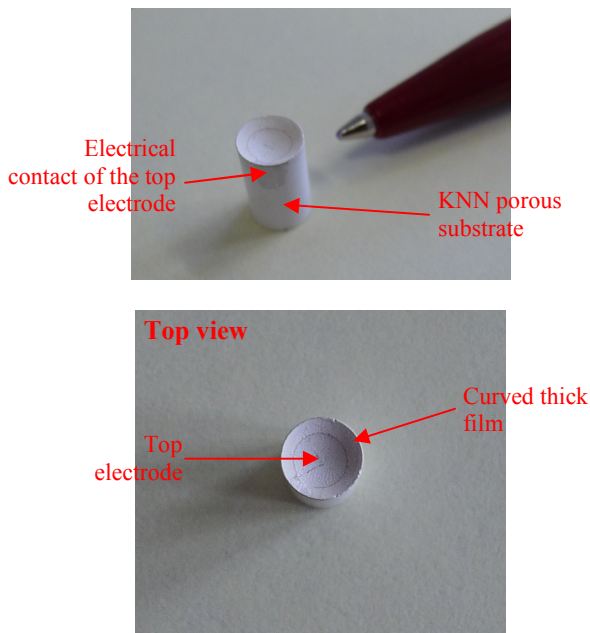


Figure 1: Photographs of the lead-free curved structure.

### 3 Structure characterization

Before the characterisation of the thick films, the acoustic properties of the porous KNN substrate used as a backing must be perfectly known. To facilitate this characterisation, larger pieces were specially fabricated (with a thickness around 10 mm and a diameter of 20 mm). With two commercial transducers (centre frequency at 2.25 MHz), a transmission method in contact was used to measure the time of flight and consequently the longitudinal wave velocity. The density was measured by Archimedes method. The values obtained are the following:

- Longitudinal wave velocity :  $v_l=3185$  m/s;
- Density :  $\rho=3580$  kg/m<sup>3</sup>;
- Acoustical impedance:  $Z=11.4$  MRa.

#### 3.1 Screen-printed thick film

Screen-printed thick films with similar KNN-based composition on alumina substrates were fabricated (Figure 2). The fabrication process was previously described in [11].

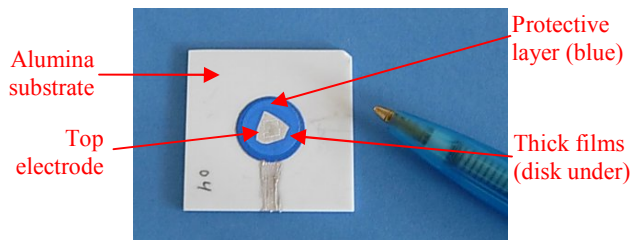


Figure 2: Photograph of a sample with screen-printed lead-free thick film on alumina substrate.

An equivalent electrical circuit model (KLM [13]) was used to simulate the the thickness mode electrical impedance

of the samples as a function of frequency. It allows to calculate and to fit the experimental data in order to obtain the thickness-mode parameters (Figure 3). The structures contain three passive layers (an alumina substrate and two electrodes) and one piezoelectric layer. The dimensions of the top electrode were large in comparison to the thickness of the piezoelectric film so that a one-dimensional thickness-mode vibration can be assumed. In these structures, the resonances in the alumina substrate were coupled with those in the piezoelectric thick film. The accuracy of the deduced piezoelectric thick-film parameters depends on the accuracy of the data for the other layers. For these three passive layers, precise data can be obtained [14] and are summarized in Table 1. Finally, with the KLM model and a fitting process on the experimental complex electrical impedance, thickness mode parameters are deduced and given in Table 2 [15].

Table 1: Acoustic characteristics of inert layers in the structure.

Inert layer	Material	parameters				
		t μm	$\rho$ kg/m <sup>3</sup>	$v_l$ m/s	Z MRa	$\alpha$ dB/m m/M Hz
Top electrode	Ag	5	10500	3600	37.8	-
Bottom electrode	Au	5	19320	3240	62.6	-
Substrate	Al <sub>2</sub> O <sub>3</sub>	1000	3900	10500	41	0.006

t: thickness;  $\rho$ : density;  $v_l$  (m/s): longitudinal wave velocity; Z: acoustical impedance;  $\alpha$ : attenuation coefficient.

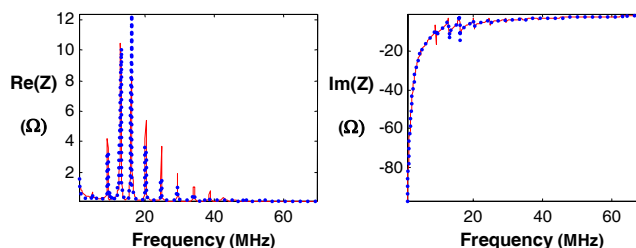


Figure 3: Real and imaginary parts of electrical impedance versus frequency of screen-printed KNN-based thick films on flat alumina substrate (red lines : theoretical, blue points : experimental).

#### 3.2 Pad-printed thick film

Using the method described in the previous paragraph, the characterization of pad-printed thick films was performed. The characteristics of the porous KNN substrate were used (at the beginning of this section 3). A cross

section of a similar structure was observed and by optical microscopy, the thickness of each layer was deduced. For the silver top and gold bottom electrodes thicknesses are 15  $\mu\text{m}$  and 6  $\mu\text{m}$  respectively (properties in Table 1). All the deduced parameters are summarized in Table 2. The piezoelectric thick film characteristics obtained by the two processes (screen-printing and pad-printing) are similar with a thickness coupling factor value equal or over 30%. For the pad-printed thick film, porosity is slightly higher which leads to a lower dielectric constant and longitudinal wave velocity (and consequently lower acoustical impedance).

Table 2: Electromechanical properties of piezoelectric thick films.

Parameters	Deposition process	
	Pad-printing	Screen-printing
A ( $\text{mm}^2$ )	12.2	6.4
t ( $\mu\text{m}$ )	50	43
$v_l$ (m/s)	2140	3360
$f_a$ (MHz)	31.4	39
$\epsilon_{33}^S / \epsilon_0$	90	140
$k_t$ (%)	34	30
$\delta_m$ (%)	15	9
Z (MRa)	11.3	11.8

A: area (top electrode); t: thickness,  $v_l$ : longitudinal wave velocity,  $f_a$ : anti-resonance frequency (if the thick film is assumed to be in free resonator conditions),  $\epsilon_{33}^S / \epsilon_0$ : dielectric constant,  $k_t$ : effective thickness coupling factor,  $\delta_m$ : mechanical losses, Z: acoustical impedance.

## 4 Transducers

### 4.1 Fabrication

The transducer fabrication procedure is relatively simple using the previously fabricated structure. The two electrical contacts on the lateral side of the backing are connected to a 50 ohm coaxial cable. The structure is inserted and glued in a polymer housing, the dimensions of which were designed to be integrated in a mechanical probe (Figure 4).

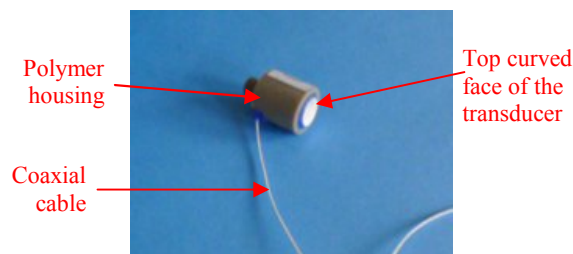


Figure 4: Photographs of the transducer.

### 4.2 Acoustic characterisation

The transducer was characterised in pulse-echo mode on a flat metallic target in water. Electrical excitation was performed with an in-house broadband generator. The pulse echo-responses (time and frequency) at the focal distance are represented in Figure 5.

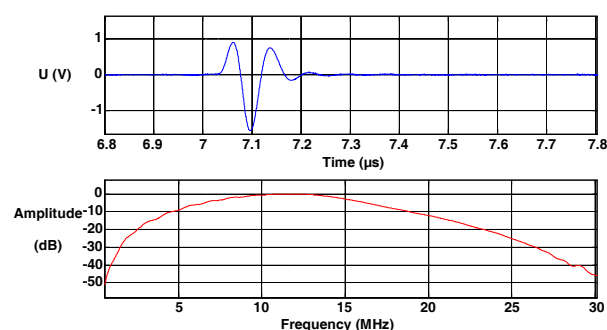


Figure 5: Experimental time (in blue) and frequency (in red) responses of the transducer at the focal distance.

The measured center frequency is at 12 MHz and the -6dB relative bandwidth is 93%. The sensitivity  $S = 20\log_{10}(U_e/U_r)$ , where  $U_e$  and  $U_r$  are the excitation and reception peak voltages, was evaluated through the measurement of the received voltage in pulse-echo mode, at  $S = -41$  dB for this transducer.

## 5 Echographic images

A real time ultrasonic scanner (ATYS MEDICAL [16]) was used to record several images of human forearm skin and nail. Previously, the lead-free transducer (Figure 4) was integrated in the probe of this high frequency echographic system. Images are presented in Figure 6. High axial and lateral resolutions allowed good image quality to be obtained despite the relatively low centre frequency. However, due to the low f-number ( $f_{\#}=1.3$  which is the ratio between the focal distance and the diameter of the top electrode), the depth of field is relatively short.

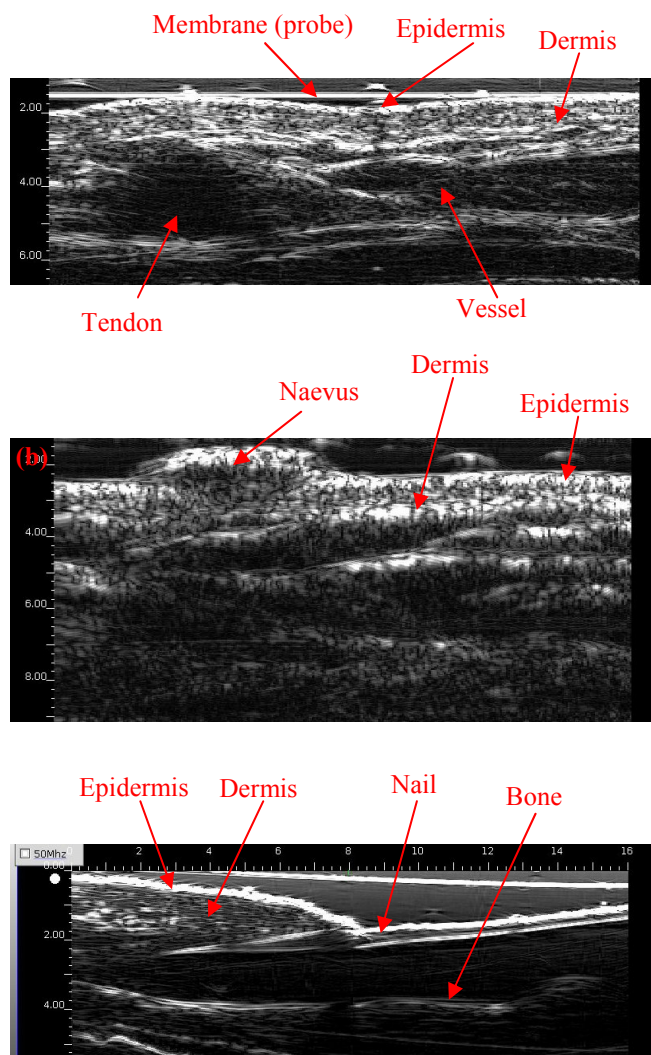


Figure 6: High resolution *in vivo* images of (a) skin and (b) naevus of human forearm, (c) nail (finger) (image dimensions are around 16mm×4mm).

## 5 Conclusion

A lead-free transducer with low f-number (1.3) was fabricated using a curved pad-printed KNN-LT thick film with sufficiently high electromechanical properties ( $k_t$  close to 35%). The centre frequency is over 10 MHz and the -6dB bandwidth is 93%, which leads to high spatial resolutions. *In vivo* echographic skin images confirm that the replacement of lead-based high frequency transducers by “green” devices can be a viable option. A transducer based on a thinner lead-free film (around 20  $\mu\text{m}$ ) to increase the resonance frequency and with a f-number of 2.5 (to have a better trade-off between lateral resolution, depth of field and sensitivity) is under fabrication to confirm that it can compete with high frequency PZT based transducers.

## Acknowledgments

The authors thank J.-Y. Tartu for transducer fabrication.

This work was partially funded by the E.U. in the FP6 NoE MIND and the PiezoInstitute (centre of European expertise and resources in piezoelectric materials and devices).

## References

- [1] Directive 2002/95/EC, on the restriction of the use of certain hazardous substances in electrical and electronic equipment, Official Journal of the European Union 13-02-2003.
- [2] T.R. Shrout, S.J. Zhang, “Lead-free piezoelectric ceramics: alternatives for PZT?”, *J. Electroceram*, 19, 111-124 (2007).
- [3] J. Rödel, W. Jo, K.T.P. Seifert, E.-M. Anton, T. Granzow, D. Damjanovic “Perspective on the development of lead-free piezoceramics”, *J. Am. Ceram Soc.*, 92(6), 1153-11177 (2009).
- [4] J. Rödel, A.B.N. Kouna, M. Weissenber-Eibl, D. Koch, A. Bierwisch, W. Rossner, M.J. Hoffmann, R. Danzer, G. Schneider, “Perspective on a roadmap for ceramic 2010 2025”, *J. Am. Ceram Soc.*, 29, 1549-1560 (2009).
- [5] E. Hollenstein, M. Davis, D. Damjanovic, N. Setter, “Piezoelectric properties of Li- and Ta-modified  $(\text{K}_{0.5}\text{Na}_{0.5})\text{NbO}_3$  ceramics,” *Appl. Phys. Letter*, 87, 182905 (2005).
- [6] D.W. Wu, R.M. Chen, Q.F. Zhou, D.M. Lin, H.L.W. Chan, K.K. Shung, “Lead-free piezoelectric ceramics for high-frequency ultrasound transducers,” *Proc. IEEE International Ultrasonics Symposium*, 2590-2593 (2007).
- [7] B. Jadidian, N.M. Hagh, A.A. winder, A. Safari, “25 MHz ultrasonic transducers with lead-free piezoceramic, 1-3 PZT fiber-epoxy composite, and PVDF polymer active elements,” *IEEE Transactions on Ultrasonics, Ferroelectrics and Frequency Control*, 56(2), 368-378 (2009).
- [8] Y. Chen, X.P. Jiang, H.S. Luo, J.Y. Dai, H.L.W. Chan, “High-frequency ultrasonic transducer fabricated with lead-free piezoelectric single crystal,” *IEEE Transactions on Ultrasonics, Ferroelectrics and Frequency Control*, 57(11), 2601-2604 (2010).
- [9] S.T.F. Lee, K.H. Lam, X.M. Zhang, H.L.W. Chan, “High-frequency ultrasonic transducer based on lead-free BSZT piezoceramics,” *Ultrasonics*, 51, 811-814 (2011).
- [10] P. Maréchal, F. Levassort, J. Holc, L.P. Tran-Huu-Hue, M. Kosec, M. Lethiecq, “High frequency transducers based on integrated piezoelectric thick films for medical imaging,” *IEEE Transactions on Ultrasonics, Ferroelectrics and Frequency Control*, 53(8), 1524-1533 (2006).
- [11] K. Hansen, K. Astafiev, T. Zawada, “Lead-free piezoelectric thick films based on potassium sodium niobate solutions,” *Proc. IEEE International Ultrasonics Symposium*, 1738-1741 (2009).
- [12] F. Levassort, E. Filoux, R. Lou-Møller, E. Ringgaard, M. Lethiecq, A. Nowicki, “Curved piezoelectric thick films for high resolution medical imaging,” *Proc.*

- IEEE International Ultrasonics Symposium*, 2361-2364 (2006).
- [13] R. Krimholtz, D.A. Leedom and G.L. Mathei, "New equivalent circuit for elementary piezoelectric transducers," *Electron. Lett.*, 38, 398-399 (1970).
- [14] A. Bardaine, P. Boy, P. Belleville, O. Acher, F. Levassort, "Improvement of composite sol-gel process for manufacturing 40  $\mu\text{m}$  piezoelectric thick films," *Journal of European Ceramic Society*, 28, 1649-1655 (2008).
- [15] F. Levassort, L.P. Tran-Huu-Hue, J. Holc, T. Bove, M. Kosec, M. Lethiecq, "High performance piezoceramic films on substrates for high frequency imaging," *Proc. IEEE International Ultrasonics Symposium*, 1035-1038 (2001).
- [16] <http://atysmedical.com/pages/produits/dermcup.php>